JVI Journals.ASM.org

Infection of Mouse Macrophages by Seasonal Influenza Viruses Can Be Restricted at the Level of Virus Entry and at a Late Stage in the Virus Life Cycle

Sarah L. Londrigan,[a,b] Kirsty R. Short,[a,b] Joel Ma,[a,b] Leah Gillespie,[a,b] Steven P. Rockman,[c] Andrew G. Brooks,[a,b] Patrick C. Reading[a,b,c]

Department of Microbiology and Immunology, University of Melbourne, Peter Doherty Institute for Infection and Immunity, Melbourne, Victoria, Australia[a]; bioCSL Limited, Parkville, Victoria, Australia[b]; WHO Collaborating Centre for Reference and Research on Influenza, Victorian Infectious Diseases Reference Laboratory, Peter Doherty Institute for Infection and Immunity, Melbourne, Victoria, Australia[c]

ABSTRACT

Airway epithelial cells are susceptible to infection with seasonal influenza A viruses (IAV), resulting in productive virus replication and release. Macrophages (MΦ) are also permissive to IAV infection; however, virus replication is abortive. Currently, it is unclear how productive infection of MΦ is impaired or the extent to which seasonal IAV replicate in MΦ. Herein, we compared mouse MΦ and epithelial cells for their ability to support genomic replication and transcription, synthesis of viral proteins, assembly of virions, and release of infectious progeny following exposure to genetically defined IAV. We confirm that seasonal IAV differ in their ability to utilize cell surface receptors for infectious entry and that this represents one level of virus restriction. Following virus entry, we demonstrate synthesis of all eight segments of genomic viral RNA (vRNA) and mRNA, as well as seven distinct IAV proteins, in IAV-infected mouse MΦ. Although newly synthesized hemagglutinin (HA) and neuraminidase (NA) glycoproteins are incorporated into the plasma membrane and expressed at the cell surface, electron microscopy confirmed that virus assembly was defective in IAV-infected MΦ, defining a second level of restriction late in the virus life cycle.

IMPORTANCE

Seasonal influenza A viruses (IAV) and highly pathogenic avian influenza viruses (HPAI) infect macrophages, but only HPAI replicate productively in these cells. Herein, we demonstrate that impaired virus uptake into macrophages represents one level of restriction limiting infection by seasonal IAV. Following uptake, seasonal IAV do not complete productive replication in macrophages, representing a second level of restriction. Using murine macrophages, we demonstrate that productive infection is blocked late in the virus life cycle, such that virus assembly is defective and newly synthesized virions are not released. These studies represent an important step toward identifying host-encoded factors that block replication of seasonal IAV, but not HPAI, in macrophages.

In humans, infection with seasonal influenza A viruses (IAV) is generally restricted to the respiratory tract. IAV infection of airway epithelial cells (AEC) is initiated following recognition of cell surface sialic acid (SIA) by the viral hemagglutinin (HA) glycoprotein (reviewed in reference 1). In addition to HA-SIA binding, it is likely that particular membrane-associated glycoproteins and/or glycolipids facilitate virus entry into AEC; however, the identity of such an entry receptor(s) is currently unknown. IAV infection of AEC results in productive virus replication, characterized by synthesis of viral RNA (vRNA) and mRNA, production of viral proteins, virion assembly, and budding of viral progeny from the surfaces of infected cells. Productive infection of AEC results in amplification of IAV in the airways, promoting virus dissemination and disease.

In addition to AEC, macrophages (MΦ) are one of the first cells in the respiratory tract to detect and respond to IAV. As for AEC, binding of the IAV HA to SIA concentrates virus at the MΦ cell surface to promote interactions with other receptors that facilitate virus entry. While IAV infection of AEC results in productive virus replication, infection of MΦ with seasonal IAV is generally considered to be abortive (reviewed in reference 2). These findings indicate that MΦ and AEC respond very differently to infection with seasonal IAV and suggest an important role for MΦ in limiting infection and disease. Consistent with this, depletion of airway MΦ has been associated with enhanced virus replication and disease in mice (3), ferrets (4), and pigs (5) following infection with seasonal IAV strains.

As MΦ can limit the severity of IAV-induced disease, virus strains that evade or exploit MΦ defenses are likely to cause severe disease. Our recent studies identified the MΦ mannose receptor (MMR) and MΦ galactose-type lectin-1 (MGL1) as attachment and entry receptors for IAV. Glycans expressed on the HA and neuraminidase (NA) surface glycoproteins of IAV are recognized by MMR and/or MGL1, promoting infectious entry into mouse MΦ (6–8). However, the mouse-virulent A/Puerto Rico/9/34 (PR8; H1N1 subtype) strain is poorly glycosylated and not recog-

Received 25 June 2015 **Accepted** 22 September 2015

Accepted manuscript posted online 30 September 2015

Citation Londrigan SL, Short KR, Ma J, Gillespie L, Rockman SP, Brooks AG, Reading PC. 2015. Infection of mouse macrophages by seasonal influenza viruses can be restricted at the level of virus entry and at a late stage in the virus life cycle. J Virol 89:12319–12329. doi:10.1128/JVI.01455-15.

Editor: A. García-Sastre

Address correspondence to Patrick C. Reading, preading@unimelb.edu.au.

nized efficiently by either receptor, consistent with its limited capacity to infect mouse MΦ *in vitro* (6, 7, 9).

At least three hypotheses have been proposed to account for the restriction of IAV replication in MΦ. First, differences between seasonal IAV in their ability to utilize cell surface receptors for viral entry suggest that impaired virus uptake into MΦ might represent one level at which virus replication is restricted. However, at least some seasonal IAV strains infect MΦ efficiently, resulting in intracellular synthesis of viral nucleoprotein (NP) and/or HA proteins (6, 7, 10), yet no infectious viral progeny are released. Thus, a block in virus assembly and/or budding may represent a second level of replication restriction in MΦ. Third, a recent study proposed that following virus internalization, a subsequent block(s) early in the virus life cycle restricted efficient nuclear entry and therefore, viral transcription and translation and ultimately, replication of seasonal IAV (11). To gain further insight regarding the extent to which viral replication proceeds and the mechanism(s) by which productive replication is blocked in MΦ, the present study has defined vRNA and mRNA synthesis for each gene segment, production of individual viral proteins, and assessment of virus assembly and release in MΦ, using epithelial cells as control cells that support productive replication of seasonal IAV. These studies confirm that impaired virus uptake into MΦ represents one level of restriction. While uptake and nuclear entry of viral RNPs can occur efficiently in IAV-infected MΦ, additional restrictions late in the virus life cycle prevented virus assembly, and therefore productive replication, in MΦ.

MATERIALS AND METHODS

Cell lines and primary macrophages. Madin-Darby canine kidney (MDCK) cells (American Type Culture Collection [ATCC], Manassas, VA) were cultured in RPMI 1640 medium (Gibco-BRL, NY) supplemented with 10% (vol/vol) fetal calf serum (JRH Biosciences, KS), 4 mM L-glutamine, 100 IU of penicillin, 10 μg of streptomycin/ml, nonessential amino acids (Gibco-BRL), and 50 μM β-mercaptoethanol. LA-4 mouse lung epithelial cells and the RAW264.7 MΦ cell line (ATCC) were cultured in Kaign's modification of Ham's F-12 medium (Gibco-BRL) and Dulbecco modified Eagle medium (DMEM) (Gibco-BRL), respectively, supplemented as described above. MDCK cells (2.5×10^4 cells/well), LA-4 cells (5×10^4 cells/well), and RAW264.7 cells (6.25×10^4 cells/well) were seeded into eight-well glass chamber slides (LabTek, Nunc, USA) and incubated overnight to form a confluent monolayer prior to use in virus infection assays.

C57BL/6 mice were bred and housed in specific-pathogen-free conditions at the Department of Microbiology and Immunology, University of Melbourne. Mice 6 to 10 weeks of age were used in experiments conducted according to the guidelines of the University of Melbourne Animal Ethics Committee. Resident peritoneal exudate cell (PEC) MΦ and bronchoalveolar lavage (BAL) fluid MΦ were obtained from C57BL/6 mice as previously described (7). MΦ (2.5×10^5 cells/well) were seeded into eight-well glass chamber slides in RPMI 1640 medium supplemented as described above and incubated for 4 h at 37°C, and the adherent MΦ population was washed to remove nonadherent cells before overnight incubation at 37°C.

Viruses. Reassortant IAV were generated by eight-plasmid reverse genetics as described previously (12). The viruses used were 7:1 reassortants consisting of the A/PR8/34 (PR8, H1N1) backbone with the HA from A/Brazil/11/78 (RG-Braz-HA) or all eight genes from PR8 (RG-PR8-HA). The rescued viruses were recovered after 3 days and amplified in the allantoic cavities of 10-day-old embryonated eggs and titrated on MDCK cells by standard procedures (13). Viruses were purified by rate zonal sedimentation on 25 to 80% (wt/vol) sucrose gradients as described previously (13).

Virus infection assays. MΦ and epithelial cells were infected with IAV, and the percentage of IAV-infected cells was determined as described previously (8, 14). Unless stated otherwise, the cells were incubated with 10^6 PFU of IAV (representing a multiplicity of infection [MOI] of 5 PFU/cell) in serum-free medium for 1 h at 37°C. Virus inoculum was removed, and the cells were washed and incubated for a further 1 to 7 h at 37°C in serum-free medium. IAV-infected cells were stained using monoclonal antibody (MAb) MP3.10g2.1C7 (WHO Collaborating Centre for Reference and Research on Influenza, Melbourne, Australia), specific for the IAV nucleoprotein (NP), followed by fluorescein isothiocyanate (FITC)-conjugated goat anti-mouse Ig (Millipore, MA). The percentage of virus-infected cells was determined by costaining with 4′,6-diamidino-2-phenylindole (DAPI) or propidium iodide (PI). A minimum of 200 cells was counted for each sample. Images were acquired with a Zeiss LSM700 confocal microscope (Zeiss, Germany) and managed using Adobe Photoshop software.

In some experiments, cells were pretreated with (i) 5 mg/ml of asialofetuin (ASF) (Sigma-Aldrich) or (ii) 10 mg/ml of mannan (Sigma-Aldrich) in serum-free medium for 30 min at 37°C to block C-type lectin receptors (CLR) prior to the addition of virus inoculum. In other experiments, virus inoculum was added in the presence of a 10 nM concentration of the NA inhibitor zanamivir (4-guanidino-2,3-dehydro-*N*-acetylneuraminic acid; purchased from GlaxoSmithKline, Australia).

Virus binding assays. The ability of IAV to bind to cells was determined by flow cytometric analysis. Briefly, cells were detached by gentle scraping in phosphate-buffered saline (PBS) with 1 mM EDTA and incubated with 10 μg/ml of purified RG-Braz-HA or RG-PR8-HA virus at 4°C for 30 min in Tris-buffered saline (TBS) containing 5 mM calcium and 1 mg/ml bovine serum albumin (BSA) (Sigma-Aldrich). Bound virus was detected using rabbit polyclonal antisera raised against N1 neuraminidase (NA) (R301, obtained from the WHO Collaborating Centre for Reference and Research on Influenza, Melbourne, Australia) in conjunction with goat anti-rabbit Ig–FITC conjugate (Millipore). Note that at 10 μg/ml, purified RG-Braz-HA or RG-PR8-HA viruses showed equivalent hemagglutinating activity using 1% turkey erythrocytes.

Virus growth assays. To determine whether infection resulted in amplification and release of infectious virus from target cells, we first performed experiments to examine release of infectious virus following a single cycle of virus replication (i.e., in the absence of exogenous trypsin). Cell monolayers in chamber slides were infected with 10^6 PFU/well (MOI of 5) of virus, as described above. Cell supernatants were collected at 2 and 24 h postinfection, and incubated with tosylsulfonyl phenylalanyl chloromethyl ketone (TPCK)-treated trypsin (4 μg/ml; Sigma, USA) for 30 min at 37°C to facilitate cleavage of viral hemagglutinin (1), before the titers of infectious virus were determined by standard plaque assay on MDCK cells.

In experiments to examine virus release following multiple cycles of virus replication, cell monolayers were infected with virus at an MOI of 0.01 and washed and cultured in serum-free medium supplemented with 1 μg/ml TPCK-treated trypsin. Cell supernatants were removed at 2, 24, and 48 h, and titers of infectious virus were determined by plaque assay on MDCK cells.

qRT-PCR for detection of host antiviral factors in IAV-infected cells. Reverse transcriptase quantitative PCR (qRT-PCR) was used to determine expression of the following host antiviral genes in mock-infected and IAV-infected cells: interferon (IFN)-induced protein with tetratricopeptide repeats 1 (IFIT1; TaqMan identifier [ID] Mm00515153_m1), IFN-induced protein with tetratricopeptide repeats 3 (IFIT3; TaqMan ID Mm01704846_s1), eukaryotic translation initiation factor 2 alpha kinase 2 (Eif2ak; TaqMan ID Mm01235643_m1), IFN induced with helicase C domain I (Ifih1 [Mda5]; TaqMan ID Mm00459183_m1), Mxyovirus resistance 1 (Mx1; TaqMan ID Mm00487796_m1), and IFN-stimulated protein 20 (Isg20; TaqMan ID Mm00469585_m1). Briefly, cell monolayers were infected as described above. At 2 or 6 h postinfection, total RNA was extracted from cells using the RNeasy minikit (Qiagen, USA) accord-

ing to the manufacturer's instructions, then treated with DNase (TURBO DNase kit; Life Technologies, Australia) to remove contaminating DNA, and stored at −70°C. Five hundred nanograms of total RNA was reverse transcribed into cDNA using the Superscript VILO cDNA synthesis kit (Life Technologies). qRT-PCR was performed using 2 ng of cDNA, TaqMan gene expression assays (Life Technologies), and TaqMan Fast Advanced mastermix on the StepOnePlus real-time PCR machine (Life Technologies). The threshold cycles (C_Ts) of gene targets determined by qRT-PCR were normalized to the geometric means of the C_Ts of three endogenous control genes, phosphoglycerate kinase 1 (Pgk1; TaqMan ID Mm00435617_m1), TATA box binding protein (Tbp; TaqMan ID Mm00446973_m1), and hypoxanthine guanine phosphoribosyltransferase (Hprt; TaqMan ID Mm00446968_m1). The relative levels of expression for each sample were determined using the $2^{-\Delta CT}$ method (15).

qRT-PCR for influenza virus mRNA and vRNA. The levels of viral RNA (vRNA) and mRNA for each IAV gene in virus-infected cells were determined by qRT-PCR. Briefly, cell monolayers were infected, and then RNA extraction and DNase treatment were performed as described above. The levels of vRNA and mRNA for the matrix (M), NP, HA, NA, polymerase acidic protein (PA), polymerase B subunit 1 (PB1), PB2, and nonstructural protein (NS) genes were determined via qRT-PCR using SYBR green-based chemistry, as described previously (16). Briefly, cDNA was synthesized using the Omniscript reverse transcriptase kit (Qiagen, USA) according to the manufacturer's instructions with oligo(dT)s (Roche, Australia) for mRNA or Uni12 primer (17) for vRNA. cDNA was then used for the real-time PCR with the SensiMIX SYBR Hi-ROX kit (Bioline, Australia) according to the manufacturer's instructions, using a Stratagene Mx3005 instrument in conjunction with MxPro software (Agilent Technologies, CA, USA). Specific primer sequences are available upon request. vRNA and mRNA copy numbers were calculated by generating a standard curve using serial dilutions of plasmid containing DNA for each IAV gene.

Western blotting for IAV proteins. Confluent cell monolayers were infected in chamber slides as described above. Whole virus-cell lysates were prepared at 2 and 16 h postinfection using a buffer comprising 50 mM Tris-HCl (pH 7.5), 150 mM NaCl, 0.5% (vol/vol) Triton X-100, 1 mM $CaCl_2$, 1 mM $MgCl_2$, and broad-spectrum protease inhibitor cocktail (Roche, Mannheim, Germany). Samples were heated to 90°C for 5 min before separation by SDS-PAGE under reducing conditions using 10 to 12.5% gels, followed by transfer to polyvinylidene difluoride (PVDF) membranes (Millipore) in Tris-glycine transfer buffer (25 mM Tris containing 192 mM glycine and 10% [vol/vol] methanol; pH 8.3). To detect IAV proteins, membranes were blocked in PBS containing 5% (wt/vol) BSA and 0.1% (vol/vol) Tween 20 (Sigma). All subsequent wash and antibody binding steps were performed in PBS containing 0.05% (vol/vol) Tween 20. Cellular β-actin (approximately 43 kDa) was monitored to ensure equivalent protein loading of all samples using a mouse monoclonal antibody to β-actin (clone sc-47778; Santa Cruz, CA, USA) in conjunction with chicken anti-mouse Ig–Alexa Fluor 488 conjugate (Life Technologies, OR, USA). IAV nonstructural protein 1 (NS1; approximately 26 kDa) and nonstructural protein 2 (NS2; approximately 14 kDa) were detected using rabbit polyclonal antibodies specific for each protein (PA5-32243 and PA5-32234, respectively, purchased from Thermo Scientific, Rockford, IL, USA) in conjunction with donkey anti-rabbit Ig–Alexa Fluor 568 conjugate (Life Technologies). IAV matrix 1 protein (M1; approximately 27 kDa) and matrix 2 protein (M2 approximately 11 kDa) were detected using mouse monoclonal antibodies to M1 (clone GA2B; Serotec) and M2 (clone 14C2; Abcam, Cambridge, United Kingdom) in conjunction with chicken anti-mouse Ig–Alexa Fluor 488 conjugate. IAV NP (approximately 46 kDa) was detected using mouse monoclonal antibody to NP (clone MP3.10g2.1C7; WHO Collaborating Centre for Reference and Research on Influenza, Melbourne, Australia) in conjunction with chicken anti-mouse Ig–Alexa Fluor 488 conjugate. Images were obtained using a Pharos FX Plus molecular imager (Bio-Rad) and managed using Adobe Photoshop software.

Fluorescence-activated cell sorting (FACS) analysis for IAV proteins. Cells were infected with IAV as described above. At 2 h and 8 h postinfection, infected cells were detached by scraping in PBS containing 1 mM EDTA. IAV HA and NA proteins expressed at the cell surface were detected using a mouse monoclonal antibody specific for H1 HA (MAb 43, obtained from the WHO Collaborating Centre for Reference and Research on Influenza, Melbourne, Australia) in conjunction with goat anti-mouse Ig–FITC conjugate (Millipore) or rabbit anti-NA polyclonal antisera (R301, obtained from the WHO Collaborating Centre for Reference and Research on Influenza, Melbourne, Australia) in conjunction with goat anti-rabbit Ig–FITC conjugate (Millipore), respectively, followed by flow cytometric analysis.

TEM. To visualize budding complexes on cell surfaces, PEC MΦ or MDCK cells were infected with 10^6 PFU (MOI of 5 PFU/cell) of RG-Braz-HA as described above. At 16 h postinfection, cells were fixed with 2.5% (vol/vol) glutaraldehyde in PBS for 30 min on ice. Washed cells were postfixed in 1% osmium tetroxide (1 h, room temperature) before being dehydrated in a graded series of ethanol solutions and embedded in Spurr's low-viscosity embedding mixture (Electron Microscopy Sciences [EMS], Hatfield, PA). Sections were cut with an ultramicrotome, collected onto coated copper grids, stained with saturated uranyl acetate for 10 min, and then triple lead stained. Sections were viewed using a Philips CM-10 transmission electron microscope (TEM) (Philips, The Netherlands) at 60 kV, and images were obtained using a Quemesa TEM camera (Olympus, Germany).

Statistical analysis. Graphing and statistical analysis of data were performed using GraphPad Prism (GraphPad Software, San Diego, CA). For comparison of multiple data sets, one-way analysis of variance (ANOVA) with Tukey's multiple comparative analysis was used. For analysis of two data sets, an unpaired two-tailed Student's *t* test was used. A P value of ≤ 0.05 was considered statistically significant in both applications.

RESULTS

Infection of mouse MΦ and epithelial cells by genetically defined strains of IAV that differ only in HA gene expression. Glycosylation of IAV HA is a critical factor modulating the ability of C-type lectin receptors (CLR) to recognize different IAV. Highly glycosylated strains infect murine MΦ more efficiently, and infection is blocked by multivalent ligands of CLR such as mannan and asialofetuin (ASF) (6–8). We aimed to generate genetically defined viruses that differed only in their HA gene, such that one expressed the HA of the highly glycosylated H1N1 strain A/Brazil/11/78 (Braz; H1N1, four potential glycosylation sites on the head of HA) and the other expressed the HA of the H1N1 strain A/Puerto Rico/8/34 (PR8; H1N1), which lacks glycosylation sites on the head of HA. While differences in glycosylation will not be the only features of the viral HA to differ between these strains, our previous studies reported that we could not rescue virus mutants expressing the PR8 HA if more than two additional glycosylation sites had been added (18). Therefore, reverse genetics was used to engineer IAV expressing seven genes from PR8 with the HA gene either from Braz (RG-Braz-HA [RG stands for reverse genetics]) or from PR8 (RG-PR8-HA).

We compared the ability of RG-Braz-HA and RG-PR8-HA to infect MDCK epithelial cells (a standard cell line for propagation of IAV) and LA-4 epithelial cells (a mouse airway epithelial cell line), as well as mouse BAL fluid MΦ, PEC MΦ, and the mouse RAW264.7 MΦ cell line. Images of RG-Braz-HA- and RG-PR8-HA-infected cells are shown in Fig. 1A. By immunofluorescence, there was little evidence of expression of IAV NP in LA-4 epithelial cells (Fig. 1Ai and Aii, top panels) or PEC MΦ (Fig. 1Ai and Aii, bottom panels) 2 h after incubation with either strain of IAV. However, IAV NP was readily detected in LA-4 epithelial cells by 8

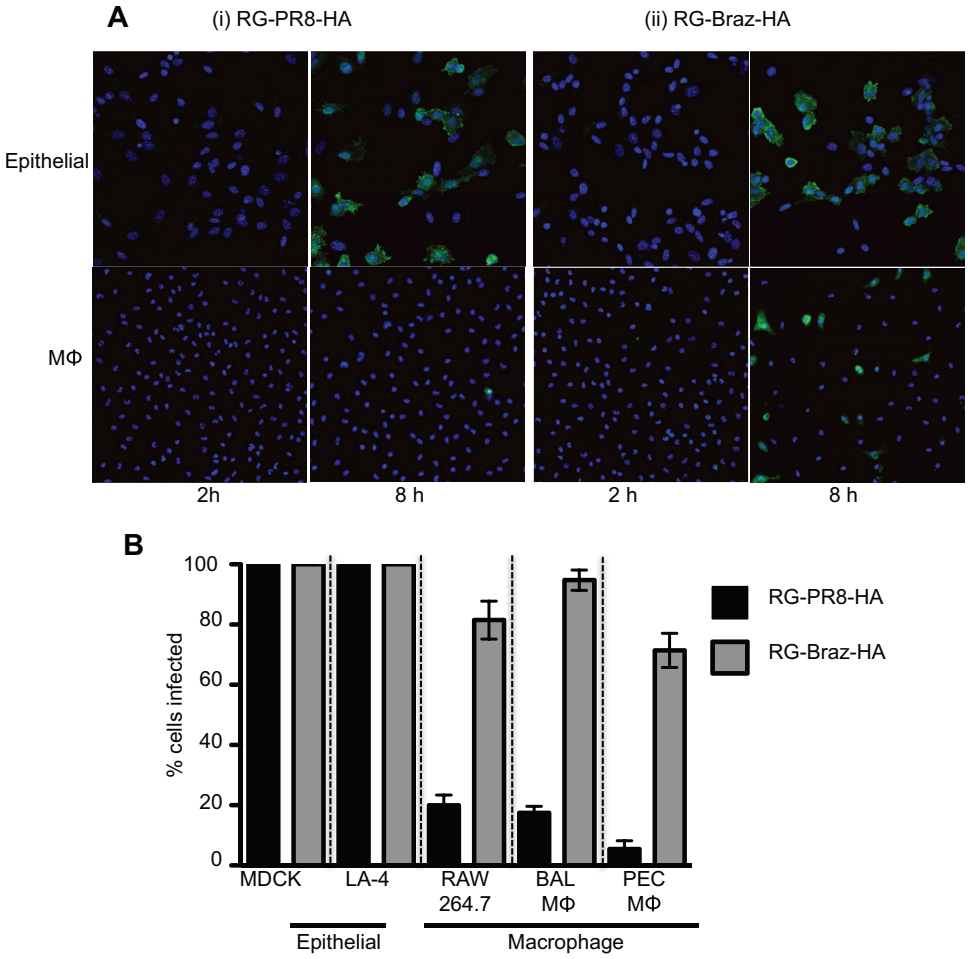

FIG 1 Differential infection of epithelial cells and mouse MΦ by genetically defined strains of IAV that differ only in HA gene expression. Monolayers of LA-4 epithelial cells (top panels) and PEC MΦ (bottom panels) were infected with an MOI of 5 PFU/cell of RG-PR8-HA or RG-Braz-HA for 1 h at 37°C. Excess virus was removed by washing, and the cells were then fixed at either 2 h or 8 h postinfection and stained by immunofluorescence for expression of newly synthesized viral NP (green) as described in Materials and Methods. DAPI staining (blue) was performed to visualize cell nuclei. (A) Viral NP^+ cells are visible at 8 h postinfection in epithelial cells infected with either RG-PR8-HA or RG-Braz-HA and only in MΦ infected with RG-Braz-HA. Magnification, ×20. (B) Monolayers of epithelial cells (MDCK and LA-4) and mouse MΦ (BAL fluid MΦ, PEC MΦ, and RAW264.7 cells) were infected with RG-PR8-HA or RG-Braz-HA as described above and then fixed at 8 h postinfection before staining by immunofluorescence to detect newly synthesized viral NP. Data represent the mean percent infection (± standard error of the mean [SEM] [error bar]) from no less than four independent fields per chamber and are representative of at least three separate experiments.

h postinfection with both RG-Braz-HA and RG-PR8-HA strains (Fig. 1Ai and Aii, top panels), consistent with detection of newly synthesized viral antigen in IAV-infected cells. IAV NP was observed only in PEC MΦ infected with RG-Braz-HA, and not RG-PR8-HA, at 8 h postinfection (Fig. 1Ai and Aii, bottom panels). Similar results were obtained using MDCK cells, BAL fluid MΦ, and RAW264.7 cells (data not shown). To determine the percentage of IAV-infected cells, PI-positive (PI^+) cells and fluorescent NP-positive (NP^+) cells were counted 7 to 8 h postinfection. RG-Braz-HA and RG-PR8-HA infected MDCK and LA-4 epithelial cells to equivalent levels (Fig. 1B), whereas only RG-Braz-HA infected mouse BAL fluid MΦ, PEC MΦ, and the RAW264.7 MΦ cell line efficiently. Consistent with published data (6–8), infection of MΦ, but not epithelial cells by IAV, was blocked by multivalent ligands of CLR (data not shown).

IAV-infected mouse epithelial cells, but not MΦ, support productive viral infection. Previously published studies report that infection of mouse MΦ with seasonal IAV results in abortive infection (7, 10, 11, 19, 20), although one study described productive replication of H1N1 IAV in mouse bone marrow-derived MΦ (21). Therefore, we investigated the ability of mouse MΦ to support productive replication of RG-Braz-HA, a virus strain that infects all mouse MΦ populations to high levels. Monolayers of mouse MΦ (PEC MΦ and RAW264.7 MΦ) and epithelial cells (MDCK cells and LA-4 cells) were incubated with 10^6 PFU (MOI of 5 PFU/cell) of RG-Braz-HA for 1 h, washed extensively to remove excess virus, and then cultured. At 2 and 24 h postinfection, supernatants were removed and clarified by centrifugation, and titers of infectious virus were determined by plaque assay on MDCK cells. As seen in Fig. 2A, RG-Braz-HA replicated productively in MDCK cells and LA-4 cells, as titers of infectious virus increased significantly between 2 h (where residual virus inoculum will be detected) and 24 h (representing virus released from infected cells). As expected, MDCK cells supported productive

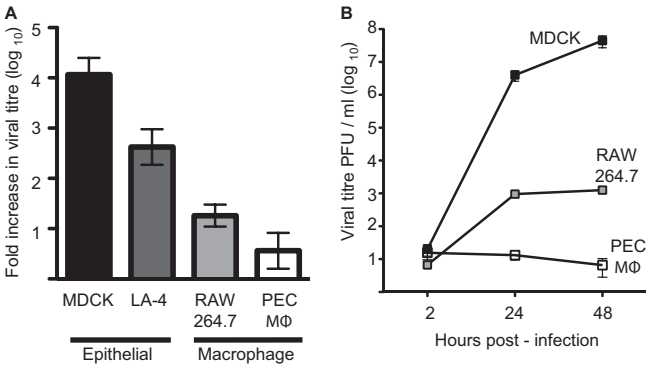

FIG 2 IAV-infected epithelial cells, but not mouse MΦ, support productive viral infection. (A) Monolayers of epithelial cells (MDCK and LA-4 cells) and mouse MΦ (PEC and RAW264.7 cells) were incubated with an MOI of 5 PFU/cell of RG-Braz-HA for 1 h, washed extensively to remove excess virus, and then cultured. At 2 and 24 h postinfection, cell culture supernatants were removed and clarified by centrifugation, and titers of infectious virus were determined by plaque assay on MDCK cells. Data represent the mean fold increase in viral titer between 2 h and 24 h postinfection (± SEM), pooled from three to five independent experiments. (B) Cell monolayers were incubated with an MOI of 0.01 PFU/cell of RG-Braz-HA for 1 h, washed extensively to remove excess virus, and then cultured in serum-free medium supplemented with 1 μg/ml TPCK-treated trypsin. At 2, 24, and 48 h postinfection, cell culture supernatants were removed and clarified by centrifugation, and titers of infectious virus were determined by plaque assay on MDCK cells. Data show the mean virus titers from triplicate samples (± SEM) in PFU per milliliter and are representative of at least two independent experiments.

replication, consistent with the widespread use of this cell line to propagate different influenza viruses *in vitro*. Although RG-Braz-HA infected mouse MΦ to high levels (Fig. 1), infection of PEC MΦ or RAW264.7 MΦ did not result in substantial increases in the amount of replication-competent virus in culture supernatants at 24 h (Fig. 2A). This phenomenon was not unique to RG-Braz-HA, as PEC MΦ were susceptible to infection but did not support productive replication, by a range of wild-type IAV H3N2 (Memphis/71, Pt Chalmers/73, and Beijing/89) and H1N1 (USSR/77, Brazil/78, and Sol Is/2006) strains (data not shown).

To investigate the potential of mouse MΦ to support growth of seasonal IAV over time, we next infected cells with a low MOI (0.01) in the presence of exogenous trypsin to facilitate cleavage of the viral HA and therefore multiple cycles of virus replication. MDCK cells supported replication of RG-Braz-HA, as titers of infectious virus released from MDCK cells increased progressively between 2, 24, and 48 h postinfection (Fig. 2B). Consistent with the data shown in Fig. 2A, mouse MΦ did not support virus replication efficiently. A modest increase in virus titers was recorded in RAW264.7 MΦ infected with RG-Braz-HA between 2 and 24 or 48 h, and the virus titers detected in supernatants from IAV-infected PEC MΦ actually declined between 2 and 24 or 48 h postinfection (Fig. 2B). Together, these results confirm that following uptake, seasonal IAV do not complete productive replication in macrophages, representing a second level of restriction.

Mouse MΦ, but not epithelial cells, differ in susceptibility and responsiveness to different IAV strains. Mouse MΦ were largely resistant to infection with RG-PR8-HA, as detected by immunofluorescence for newly synthesized viral NP at 7 to 8 h postinfection. Therefore, we hypothesized that MΦ would sense and respond to infection with RG-Braz-HA more efficiently than to RG-PR8-HA. To test this, we used qRT-PCR to measure expression of host antiviral factors in mouse MΦ and epithelial cells after infection with RG-Braz-HA or RG-PR8-HA. PEC MΦ and LA-4 mouse epithelial cells in eight-well chamber slides were mock infected or infected with 10^6 PFU (MOI of 5 PFU/cell) of RG-Braz-HA or RG-PR8-HA, and at 2 h or 6 h postinfection, cells were lysed, and RNA was extracted. The RNA was used as a template for reverse transcriptase quantitative PCR as described in Materials and Methods.

Mouse LA-4 epithelial cells upregulated expression of IFIT3, IFIT1, and Eif2ak2 in response to RG-Braz-HA and RG-PR8-HA, whereas mouse PEC MΦ responded only to RG-Braz-HA (Fig. 3, top panels). Mda5, Mx1, and Isg20 were also strongly upregulated in mouse MΦ infected with RG-Braz-HA, but not RG-PR8-HA, whereas either virus induced only modest expression of these factors in epithelial cells (Fig. 3, bottom panels). Expression of each of the host factors tested was negligible in mock-infected mouse MΦ and epithelial cells. Thus, the susceptibility of mouse MΦ and epithelial cells to infection correlates with their ability to sense and respond to different IAV as assessed by induction of host antiviral genes. Moreover, while mouse MΦ show major differences in susceptibility and responsiveness to different IAV, epithelial cells do not.

Enhanced infection of mouse MΦ by RG-PR8-HA following inhibition of the viral NA. RG-Braz-HA expresses seven genes from PR8, implicating features of the PR8 HA in the poor ability of RG-PR8-HA to infect mouse MΦ. Reduced HA-mediated attachment to sialylated receptors and/or inefficient interactions with appropriate entry receptors on the surface of MΦ could limit RG-PR8-HA infection. Alternatively, the PR8 HA may not fuse efficiently with MΦ endosomal membranes, resulting in degradation rather than infection following virus uptake. To discriminate between these possibilities, we first examined the ability of each virus to bind to the MΦ cell surface. Compared to RG-Braz-HA, there was no major difference in the ability of RG-PR8-HA to bind to the MΦ cell surface at 4°C (Fig. 4Ai and Aii); however, at this temperature, the IAV NA will not be enzymatically active as it would be in infection assays. Therefore, we infected mouse MΦ with RG-PR8-HA and RG-Braz-HA in the presence or absence of the NA inhibitor zanamivir. As seen in Fig. 4Bi, low levels of MΦ infection by RG-PR8-HA were markedly enhanced in the presence of zanamivir, and infection was blocked by mannan and/or ASF, consistent with CLR-mediated infection. Infection of MΦ by RG-Braz-HA was slightly enhanced in the presence of zanamivir, but this was not significant (Fig. 4Bii). Thus, mouse MΦ are not inherently resistant to RG-PR8-HA; instead, features of the PR8 HA (e.g., lack of glycosylation and/or avidity for SIA receptors on MΦ) and NA (e.g., ability to cleave SIA) limit infectious entry under normal circumstances. Inactivation of the viral NA appeared to enhance interactions between cell surface SIA and PR8 HA, promoting virus uptake and therefore more efficient infection of mouse MΦ by RG-PR8-HA. Therefore, impaired virus uptake into macrophages represents one level of restriction limiting infection by seasonal IAV.

Viral mRNA and vRNA for each gene segment are produced in mouse MΦ infected with seasonal IAV. To determine at what stage of the virus life cycle productive replication is blocked in MΦ, we first performed quantitative assessment of all eight gene segments of the viral RNA (vRNA) genome, as well as their transcription into mRNA. Monolayers of mouse MΦ (PEC) and epithelial cells (MDCK and LA-4 cells) were incubated with 10^6 PFU

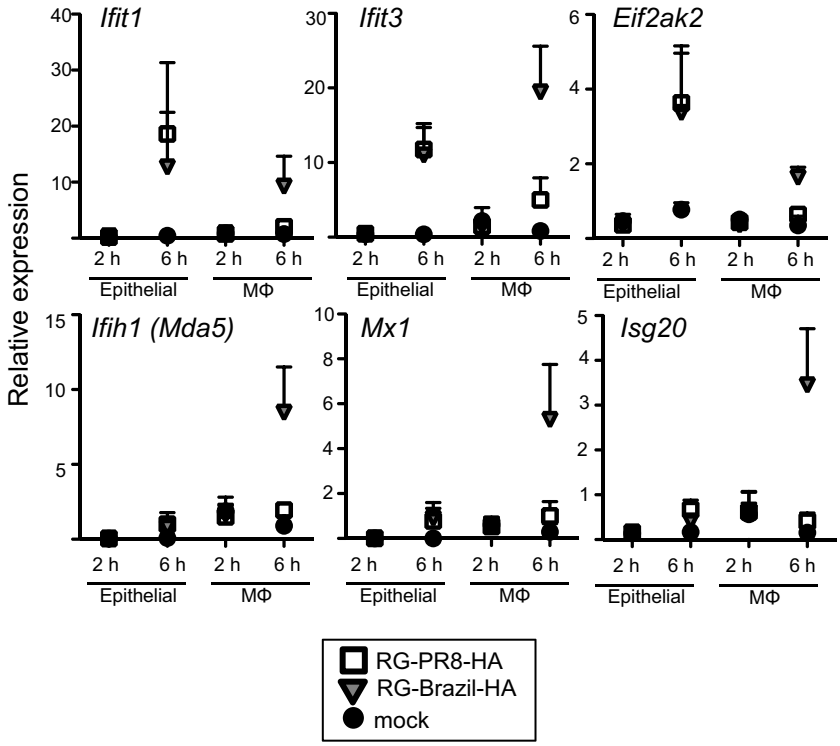

FIG 3 Mouse MΦ, but not epithelial cells, differ in susceptibility and responsiveness to different IAV strains through the induction of host antiviral factors. Monolayers of mouse LA-4 epithelial cells and PEC MΦ were infected with an MOI of 5 PFU/cell of RG-PR8-HA or RG-Braz-HA or mock infected for 1 h at 37°C. Monolayers were washed to remove excess virus, and then cells were lysed, and total RNA was extracted at 2 h or 6 h postinfection. The levels of host antiviral genes *Ifit1*, *Ifit3*, and *Eif2ak2* (top panels), as well as *Ifih1*, *Mx1*, and *Isg20* (bottom panels) were determined by qRT-PCR using TaqMan gene expression assays as described in Materials and Methods. For each gene of interest, relative gene expression (± 1 standard deviation [SD]) was determined using the $2^{-\Delta CT}$ method described in Materials and Methods, and data were pooled from three independent experiments.

(MOI of 5 PFU/cell) of RG-Braz-HA for 1 h at 37°C and washed extensively, and total RNA was isolated at 2 and 6 h postinfection. Total cellular RNA was then used as the template in a strand-specific qRT-PCR to detect negative-sense genomic vRNA and viral mRNA. Between 2 and 6 h postinfection, the levels of vRNA and mRNA of all gene segments increased markedly in IAV-infected MDCK and LA-4 cells, as well as in mouse MΦ (Fig. 5). The 2-h time point was included to account for residual virus that may have entered cells but not replicated and/or remained attached to the cell surface. Overall, there were no major defects in the synthesis of any particular segments in mouse MΦ, although vRNA/mRNA levels of each gene segment had a tendency to be somewhat lower in MΦ than in epithelial cells at both 2 h and 6 h. Together, these data indicate that vRNA and mRNA for all eight segments of the IAV genome are synthesized in mouse MΦ infected with seasonal IAV.

Expression of IAV proteins in mouse MΦ and epithelial cells infected with seasonal IAV. Previous studies have reported synthesis of viral HA, M, and NP in IAV-infected mouse MΦ (7, 10, 21); however, a comprehensive analysis of IAV proteins expressed in these cells has not been performed. Therefore, we used Western blotting to detect different IAV proteins in lysates from IAV-infected MΦ. Epithelial cells were included as positive controls, as all viral proteins should be expressed in cells that support productive virus replication. Briefly, monolayers of MΦ, LA-4, or MDCK cells were incubated with 10^6 PFU (MOI of 5 PFU/cell) of RG-Braz-HA for 1 h at 37°C and washed to remove the inoculum, and total cell lysates were prepared at 2 h (to detect input virus) and 16 h (to detect newly synthesized viral proteins) postinfection. Mock-infected cells were included for comparison, and actin protein levels were monitored in all assays to control for any differences in loading between samples.

We did not detect significant expression of any viral protein tested at 2 h postinfection in IAV-infected MDCK and LA-4 cells (Fig. 6A); however, at 16 h, nonstructural proteins (NS1 and NS2) and a number of virion-associated proteins (M1, M2, and NP) were all expressed, consistent with *de novo* synthesis in virus-infected cells. At 16 h postinfection, the level of each viral protein was generally higher in MDCK cells than in LA-4 cells, consistent with the ability of MDCK cells to support much higher levels of productive replication (Fig. 2). In IAV-infected MΦ, viral proteins NS1/NS2 and M1/M2/NP were also detected at 16 h postinfection (Fig. 6A), albeit at variable levels.

Efficient transport of the IAV HA and NA to the surfaces of host cells is important for virus morphogenesis and budding and for release of nascent virions from infected cells after budding. Flow cytometry confirmed upregulated expression of HA and NA on the surfaces of IAV-infected epithelial cells and MΦ between 2 and 8 h postinfection (Fig. 6B). The enzymatic activity of the viral NA removes SIA from infected host cells and from HA/NA glycoproteins on virions, promoting effective virus release and preventing aggregation (reviewed in reference 22). However, culture of IAV-infected MΦ with exogenous neuraminidase from *Vibrio cholerae* (100 mU/ml) did not liberate newly synthesized infec-

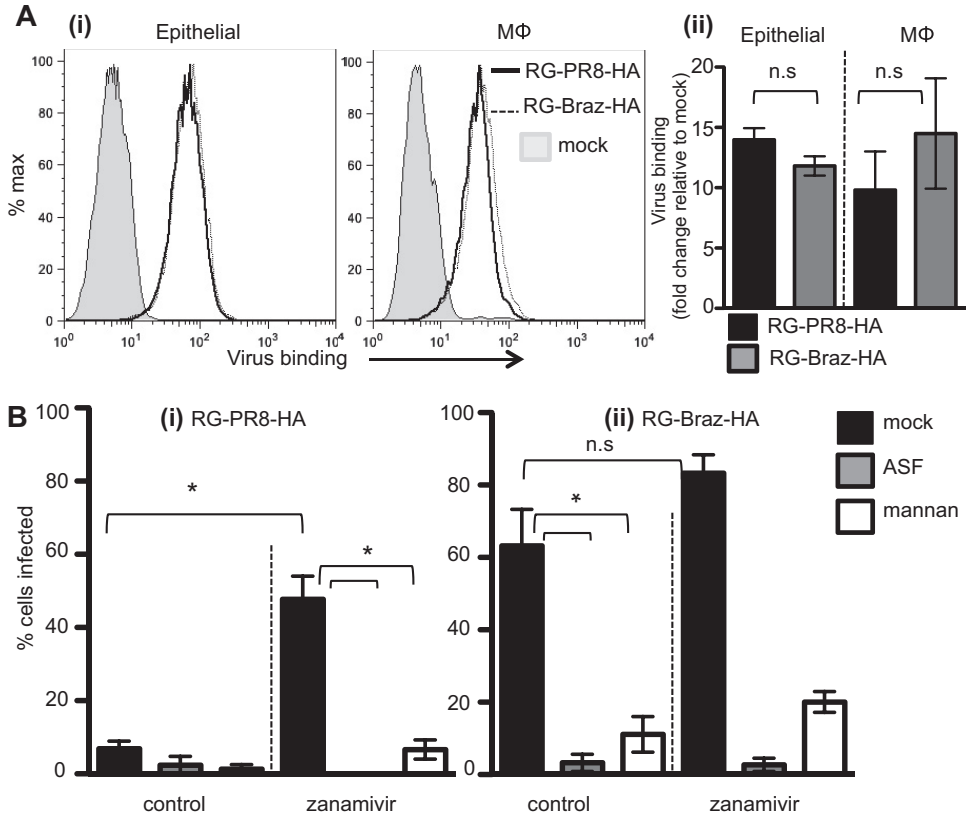

FIG 4 Both RG-PR8-HA and RG-Braz-HA bind to epithelial cells and mouse MΦ; however, inhibition of the viral NA results in enhanced infection of mouse MΦ by RG-PR8-HA. (A) Epithelial cells (MDCK) and mouse MΦ (RAW264.7) were incubated with 10 μg/ml of purified RG-PR8-HA and RG-Braz-HA or no virus (mock infected) for 30 min on ice. After the cells were washed, virus bound to the cell surface was detected using anti-NA polyclonal rabbit sera in conjunction with goat anti-rabbit Ig–FITC conjugate, followed by flow cytometry. (i) Representative histograms show binding of RG-PR8-HA and RG-Braz-HA to epithelial cells and MΦ. Staining of mock-infected cells are displayed as solid gray histograms. (ii) Data are expressed as the mean fold change (± SEM) in the geometric means of RG-PR8-HA or RG-Braz-HA bound to the cell surface relative to the geometric mean of the no-virus (mock) control. The data show pooled triplicate samples from three independent experiments. There was no significant difference (n.s) in the level of RG-PR8-HA compared with RG-Braz-HA bound to epithelial cells ($P = 0.16$) or MΦ ($P = 0.45$) (two-tailed Student's *t* test). (B) Monolayers of mouse MΦ (PEC) were infected with 10^7 PFU (MOI of 50 PFU/cell) of RG-PR8-HA or 10^6 PFU (MOI of 5 PFU/cell) of RG-Braz-HA for 1 h at 37°C in the presence or absence (control) of 10 nM zanamivir. Prior to infection, cells were also treated with 10 mg/ml mannan or 5 mg/ml asialofetuin (ASF) or mock treated to block CLR-virus interactions. Monolayers were then washed and incubated for a further 6 to 7 h in the presence or absence of zanamivir with either mannan or ASF or mock treatment. Cells were fixed and stained by immunofluorescence to detect expression of newly synthesized viral NP. Data represent the mean percent infection (± SEM) from no less than four independent fields per chamber and are representative of two independent experiments. Values that were significantly different ($P < 0.05$ by one-way ANOVA with Tukey's posthoc analysis) are indicated by bar and asterisk. Values that were not significantly different ($P > 0.05$) are indicated by a bar and n.s.

tious virus from the surfaces of IAV-infected MΦ (data not shown). Thus, while newly synthesized HA/NA glycoproteins are expressed on the surfaces of IAV-infected MΦ, defective release of nascent virions from the cell surface is not responsible for the block in productive IAV replication in MΦ.

Virus buds from the surfaces of IAV-infected epithelial cells, but not IAV-infected MΦ. For productive IAV replication to occur, vRNA is replicated in the nucleus before associating with NP and the RNA polymerase subunits (PA, PB1, and PB2) such that the assembled viral RNPs (vRNPs) exit the nucleus and traffic along microtubules to the plasma membrane (23). Assembly of IAV at the plasma membrane is a complex process, involving extensive interplay between multiple viral proteins before budding virions are pinched off and released from the infected cell. Therefore, transmission electron microscopy (TEM) was used to visualize virus at the surfaces of IAV-infected MΦ to determine whether virions formed at the cell surface were unable to complete the budding process. In these studies, monolayers of PEC MΦ or MDCK epithelial cells were infected with 10^6 PFU (MOI of 5 PFU/cell) of RG-PR8-HA and washed, and at 16 h postinfection, the cells were fixed and examined by TEM as described in Materials and Methods. As seen in Fig. 7, virus budding was readily observed from the surfaces of epithelial cells, consistent with release of infectious virus and productive IAV infection in these cells. However, we did not observe any evidence of virus budding at the plasma membrane of IAV-infected MΦ in any sections examined.

DISCUSSION

Data presented herein demonstrate that interactions between seasonal IAV and mouse MΦ can be restricted at two levels. The first restriction, at the level of virus attachment and entry, relates to the poor capacity of particular IAV to recognize appropriate attachment factors (SIA) and entry receptors (CLR) on the surfaces of MΦ. RG-PR8-HA infected mouse MΦ poorly, resulting in limited synthesis of viral NP and little "sensing" of viral infection, as implied by the modest induction of antiviral host genes. This is not

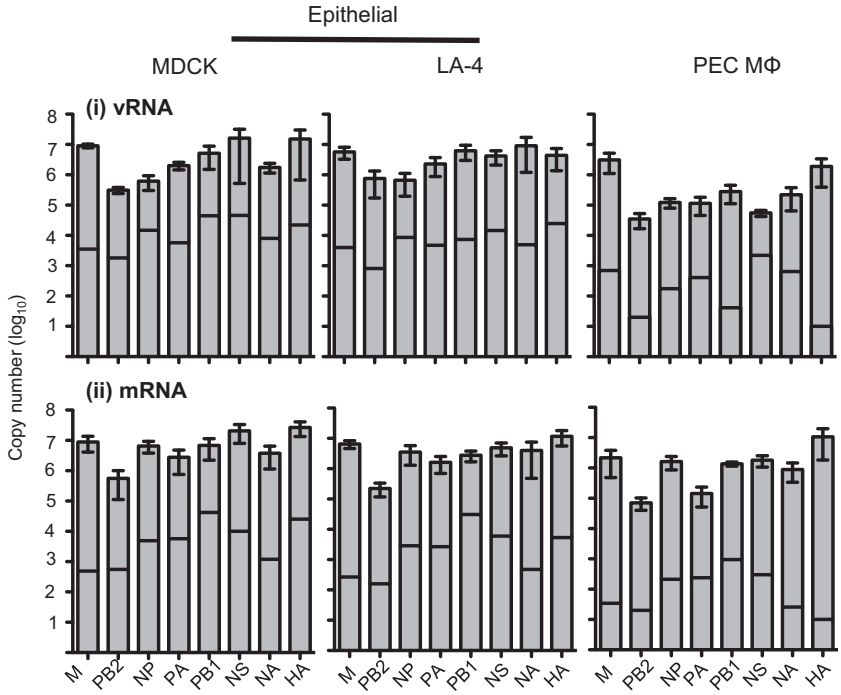

FIG 5 Viral mRNA and vRNA for each gene segment is produced in mouse MΦ and epithelial cells infected with RG-Braz-HA. Monolayers of mouse MΦ (PEC MΦ) and epithelial cells (MDCK and LA-4 cells) were incubated with an MOI of 5 PFU/cell of RG-Braz-HA for 1 h at 37°C, washed, and incubated further until total RNA was extracted 2 and 6 h postinfection. The levels of vRNA and mRNA for each IAV gene were determined via qRT-PCR as described in Materials and Methods. Data are expressed as the mean copy number (± SEM) at 6 h postinfection for each IAV gene, pooled from three independent experiments. The copy number at 2 h postinfection for each gene is represented as a horizontal line on each bar.

likely to reflect differences in stability and/or degradation of NP or other viral proteins, since RG-Braz-HA and RG-PR8-HA differ only in the HA that is expressed. While PR8 HA binds preferentially to α2,3-linked SIA and mouse MΦ express α2,6-linked SIA, resialylation of MΦ to express α2,3-linked SIA restored susceptibility to CLR-mediated infection by PR8 (24). Herein, RG-PR8-HA infected mouse MΦ to high levels in the presence of the neuraminidase inhibitor zanamivir, and infection was blocked by multivalent ligands of CLR. In both instances, enhanced binding to cell surface SIA promoted interactions between the poorly glycosylated PR8 HA and CLR on MΦ, resulting in infectious entry and detection of viral NP 6 to 8 h postinfection. These data imply no major defects in the ability of the PR8 HA to fuse with endosomal membranes or commence viral replication but instead imply that attachment and entry into MΦ are not efficient under normal circumstances.

The second level of restriction refers to the inability of seasonal IAV to complete productive replication in MΦ. Thus, RG-Braz-HA IAV infected mouse MΦ to high levels, but no infectious progeny were released. Chan et al. reported upregulation of M mRNA and protein during productive replication of seasonal IAV in mouse bone marrow-derived MΦ (21), and synthesis of HA and NP proteins has been reported during nonproductive replication in mouse MΦ (7, 10). To our knowledge, the current study is the first to examine the synthesis of viral mRNA and vRNA corresponding to all segments of the IAV genome during nonproductive replication of IAV in MΦ. Our data clearly demonstrate that new copies of vRNA and viral mRNA corresponding to each genome segment were synthesized in IAV-infected mouse MΦ. Moreover, we demonstrate synthesis of nonstructural proteins (NS1 and NS2) and virion-associated proteins (NP, HA, NA, M1, and M2), with abundant expression of HA and NA on the surfaces of IAV-infected MΦ. While our studies detected the majority of viral proteins, they do not shed light on whether the proteins are present in sufficient quantities and ratios or provide information regarding appropriate protein stability and/or localization to facilitate virus assembly. For example, abortive replication of IAV in L929 cells was associated with low levels of M1 protein (25), whereas overproduction of M2 protein was associated with nonproductive infection in Vero cells (26). Furthermore, viral proteins are subject to various posttranslational modifications (reviewed in references 27 to 29), including glycosylation (HA/NA), palmitoylation (HA and M2), SUMOylation (i.e., conjugation with the small ubiquitin-like modifier; M1, NS1, NP, PB1, and NS2), and phosphorylation (M1, NP, NS1, PB1, and PB1-F2), and modulation of these processes in IAV-infected MΦ might also affect stability and/or function of particular viral proteins.

While not examined in our study, defective synthesis and/or degradation of one or more of the viral polymerase proteins (PA, PB1, and PB2) might also limit IAV replication in MΦ at a late stage in the virus life cycle. For example, specific mutations in the viral PA were shown to abrogate IAV replication in epithelial cells despite expression of PA RNA products (30), leading the authors to propose that PA may be influencing virus assembly and/or release by an unknown mechanism(s). Given that polymerase trimers are bound to each vRNA segment in the virion core, perturbations of PA, PB1, or PB2 may also disrupt the structural integrity of the core. Note that PB1-F2 expression was not examined and while deletion mutants indicate that this viral protein is not essential for IAV replication in cell culture and mice (31, 32), we cannot

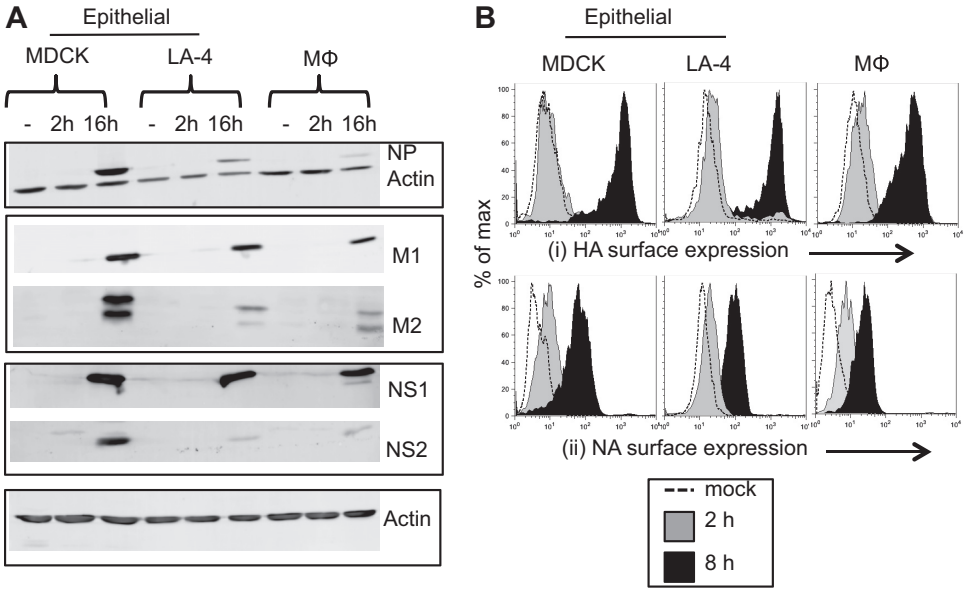

FIG 6 Expression of IAV proteins in epithelial cells and MΦ infected with RG-Braz-HA. (A) Monolayers of mouse MΦ (RAW264.7 cells) and epithelial cells (LA-4 and MDCK cells) were incubated with an MOI of 5 PFU/cell of RG-Braz-HA or no virus (−) for 1 h at 37°C and washed to remove excess virus. At 2 h and 16 h postinfection, total cell lysates were prepared, resolved by SDS-PAGE under reducing conditions, and transferred to a PVDF membrane. IAV proteins from infected cells were detected by Western blotting, using antibodies specific for each viral protein. β-Actin (approximately 42 kDa) was monitored to ensure equivalent loading between samples. Proteins of the predicted molecular mass were detected using anti-IAV antibodies specific for NP (56 kDa), M1 (27 kDa), M2 (doublet, approximately 11 kDa), NS1 (26 kDa), and NS2 (14 kDa) in epithelial cells and MΦ at 16 h postinfection. Data are representative of at least three independent samples. (B) Monolayers of mouse MΦ (RAW264.7 cells) and epithelial cells (LA-4 and MDCK cells) were incubated with an MOI of 5 PFU/cell of RG-Braz-HA or no virus (mock) for 1 h at 37°C and washed to remove excess virus. At 2 h and 8 h postinfection, viral HA and viral NA expressed on the cell surface was detected using HA-specific and NA-specific antibodies, respectively, in conjunction with flow cytometry. Data are representative of duplicate experiments.

rule out the possibility that altered PB1-F2 expression might also contribute to abortive IAV replication in MΦ.

IAV assembly and budding are complex, multistep processes that occur in lipid raft domains on the apical surfaces of infected cells (reviewed in reference 33). Clustering of HA and NA in lipid rafts has been implicated in inducing deformation of the plasma membrane and the initiation of virus budding. Flow cytometry demonstrated that HA and NA were clearly transported to the surfaces of IAV-infected MΦ, yet TEM revealed a complete absence of membrane-associated viral particles. This contrasts abortive IAV infection in HeLa cells where virus particles assembled, but were not released, from the plasma membrane (34). Rather, it has similarities with abortive IAV replication in L929 cells, where both HA and NA were synthesized and transported to the plasma membrane, but deficient M protein synthesis resulted in defective virus assembly (25). Thus, while we have not defined the precise block in productive infection of seasonal IAV in mouse MΦ, our data support the concept of a block in virus assembly prior to budding from the surfaces of infected cells.

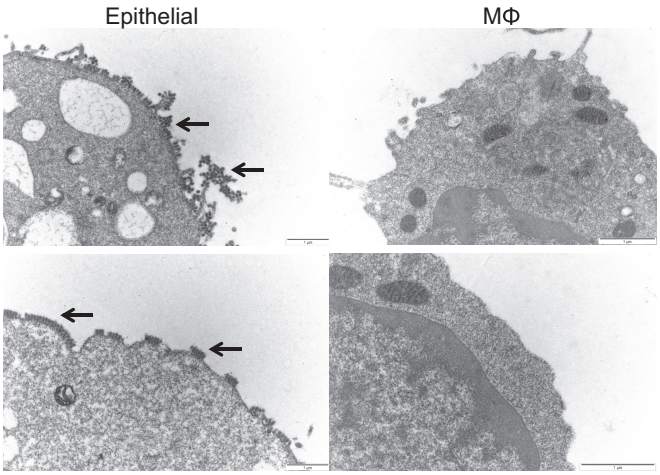

FIG 7 Virus budding from RG-Brazil-HA-infected epithelial cells but not mouse MΦ. Monolayers of mouse MΦ (PEC) and epithelial cells (MDCK cells) were incubated with an MOI of 5 PFU/cell of RG-Braz-HA for 1 h at 37°C, washed to remove excess virus, and cultured. At 16 h postinfection, cells were fixed and examined by TEM as described in Materials and Methods. Virions and densely stained particles budding from the plasma membrane of epithelial cells (indicated by black arrows), but not from mouse MΦ, can be observed.

Recent studies have identified a number of host antiviral restriction factors that limit intracellular replication of a range of viruses, including IAV. As interferon-stimulated genes (ISGs), such as human myxovirus resistance gene A (MxA), block multiple steps in viral RNA replication (35, 36), they are unlikely to be the major factors regulating nonproductive replication in MΦ, as vRNPs enter the nucleus efficiently and promote transcription and replication of viral genes. Similarly, IFN-inducible transmembrane 3 (IFITM-3) limits replication of IAV and other enveloped viruses in epithelial cells (reviewed in reference 37) by preventing cytosolic entry (38), and IAV replication in MΦ is blocked later in the virus life cycle. In epithelial cells, tetherin (also named BST-2) and viperin have been implicated in limiting release of nascent virions from the plasma membrane (39–41); however, our data

indicate that nonproductive replication in MΦ is restricted prior to the development of virus buds. Thus, while studies have implicated particular ISGs in limiting IAV infection of epithelial cells, the factors that block productive IAV replication in MΦ are not known.

Mda5, Mx1, and Isg20 were strongly upregulated in IAV-infected MΦ but not epithelial cells, suggesting cell-specific differences in the induction of these antiviral host factors. Similarly, transcripts for NLRP3, together with its adaptor protein pyrin domain (PYD)- and caspase activation and recruitment domain (CARD)-containing protein (PYCARD) were highly expressed in MΦ, but not in AEC, from naive mice, and IAV infection induced differential regulation of these genes in each cell type (42). Viperin$^{-/-}$ MΦ and DC, but not neurons or fibroblasts, showed enhanced permissivity to West Nile virus (WNV) replication (43), consistent with the notion that the antiviral roles of particular host factors can be cell specific. Moreover, identification of ISGs differentially regulated in WNV-permissive and WNV-nonpermissive neurons allowed for ectopic expression of candidate ISGs in permissive neurons to identify three genes that conferred antiviral activity against WNV, but not against unrelated alphaviruses (44). A broader understanding of the different ISGs and host genes induced in response to seasonal IAV in MΦ and epithelial cells will be an important step toward identifying specific factors that block IAV replication in MΦ, presumably by regulating the synthesis and/or stability of specific viral proteins and/or by interfering with the process of virus assembly.

For the purposes of this study, we have used genetically defined IAV representative of seasonal IAV and which, like seasonal IAV, do not replicate productively in mouse MΦ. A recent study reported that murine MΦ-supported productive replication by HPAI H5N1 and reassortant viruses expressing individual H5N1 genes in the context of seasonal IAV demonstrated that overcoming the "block" in productive replication mapped exclusively to the HA gene of HPAI H5N1 (11). Currently, the features of the HPAI H5 HA that allow these viruses to replicate in mouse MΦ have not been elucidated; however, these findings suggest that MΦ express all appropriate cellular factors and machinery to support IAV growth. Moreover, they imply that HPAI H5N1 evade cellular restriction factors that block the replication of seasonal IAV in MΦ. Ongoing experiments in the laboratory aim to identify the specific host cell factors that restrict replication of seasonal IAV in MΦ.

ACKNOWLEDGMENTS

Plasmid vectors containing each of the PR8 genes used to generate RG viruses were kindly provided by Robert Webster, St. Jude Children's Research Hospital (Memphis, TN, USA). We thank Ross Hamilton and Stephen Asquith (bioCSL) for assistance with TEM. We are grateful to Yi-Mo Deng (Melbourne WHO Collaborating Centre for Reference and Research on Influenza) for assistance with qRT-PCR of IAV genes.

This study was supported by project grants 1027545 and 1083307 from the National Health and Medical Research Council (NHMRC) of Australia. P.C.R., S.L.L., and A.G.B are all recipients of funding from the NHMRC. The Melbourne WHO Collaborating Centre for Reference and Research on Influenza is supported by the Australian Government Department of Health.

REFERENCES

1. **Skehel JJ, Wiley DC.** 2000. Receptor binding and membrane fusion in virus entry: the influenza hemagglutinin. Annu Rev Biochem **69:**531–569. http://dx.doi.org/10.1146/annurev.biochem.69.1.531.
2. **Short KR, Brooks AG, Reading PC, Londrigan SL.** 2012. The fate of influenza A virus after infection of human macrophages and dendritic cells. J Gen Virol **93:**2315–2325. http://dx.doi.org/10.1099/vir.0.045021-0.
3. **Tate MD, Pickett DL, van Rooijen N, Brooks AG, Reading PC.** 2010. Critical role of airway macrophages in modulating disease severity during influenza virus infection of mice. J Virol **84:**7569–7580. http://dx.doi.org/10.1128/JVI.00291-10.
4. **Kim HM, Kang YM, Ku KB, Park EH, Yum J, Kim JC, Jin SY, Lee JS, Kim HS, Seo SH.** 2013. The severe pathogenicity of alveolar macrophage-depleted ferrets infected with 2009 pandemic H1N1 influenza virus. Virology **444:**394–403. http://dx.doi.org/10.1016/j.virol.2013.07.006.
5. **Kim HM, Lee YW, Lee KJ, Kim HS, Cho SW, van Rooijen N, Guan Y, Seo SH.** 2008. Alveolar macrophages are indispensable for controlling influenza viruses in lungs of pigs. J Virol **82:**4265–4274. http://dx.doi.org/10.1128/JVI.02602-07.
6. **Upham JP, Pickett D, Irimura T, Anders EM, Reading PC.** 2010. Macrophage receptors for influenza A virus: role of the macrophage galactose-type lectin and mannose receptor in viral entry. J Virol **84:**3730–3737. http://dx.doi.org/10.1128/JVI.02148-09.
7. **Reading PC, Miller JL, Anders EM.** 2000. Involvement of the mannose receptor in infection of macrophages by influenza virus. J Virol **74:**5190–5197. http://dx.doi.org/10.1128/JVI.74.11.5190-5197.2000.
8. **Ng WC, Liong S, Tate MD, Irimura T, Denda-Nagai K, Brooks AG, Londrigan SL, Reading PC.** 2014. The macrophage galactose-type lectin can function as an attachment and entry receptor for influenza virus. J Virol **88:**1659–1672. http://dx.doi.org/10.1128/JVI.02014-13.
9. **Reading PC, Whitney PG, Pickett DL, Tate MD, Brooks AG.** 2010. Influenza viruses differ in ability to infect macrophages and to induce a local inflammatory response following intraperitoneal injection of mice. Immunol Cell Biol **88:**641–650. http://dx.doi.org/10.1038/icb.2010.11.
10. **Rodgers B, Mims CA.** 1981. Interaction of influenza virus with mouse macrophages. Infect Immun **31:**751–757.
11. **Cline TD, Karlsson EA, Seufzer BJ, Schultz-Cherry S.** 2013. The hemagglutinin protein of highly pathogenic H5N1 influenza viruses overcomes an early block in the replication cycle to promote productive replication in macrophages. J Virol **87:**1411–1419. http://dx.doi.org/10.1128/JVI.02682-12.
12. **Neumann G, Watanabe T, Ito H, Watanabe S, Goto H, Gao P, Hughes M, Perez DR, Donis R, Hoffmann E, Hobom G, Kawaoka Y.** 1999. Generation of influenza A viruses entirely from cloned cDNAs. Proc Natl Acad Sci U S A **96:**9345–9350. http://dx.doi.org/10.1073/pnas.96.16.9345.
13. **Anders EM, Hartley CA, Jackson DC.** 1990. Bovine and mouse serum beta inhibitors of influenza A viruses are mannose-binding lectins. Proc Natl Acad Sci U S A **87:**4485–4489. http://dx.doi.org/10.1073/pnas.87.12.4485.
14. **Londrigan SL, Tate MD, Brooks AG, Reading PC.** 2012. Cell-surface receptors on macrophages and dendritic cells for attachment and entry of influenza virus. J Leukoc Biol **92:**97–106. http://dx.doi.org/10.1189/jlb.1011492.
15. **Livak KJ, Wills QF, Tipping AJ, Datta K, Mittal R, Goldson AJ, Sexton DW, Holmes CC.** 2013. Methods for qPCR gene expression profiling applied to 1440 lymphoblastoid single cells. Methods **59:**71–79. http://dx.doi.org/10.1016/j.ymeth.2012.10.004.
16. **Short KR, Reading PC, Brown LE, Pedersen J, Gilbertson B, Job ER, Edenborough KM, Habets MN, Zomer A, Hermans PW, Diavatopoulos DA, Wijburg OL.** 2013. Influenza-induced inflammation drives pneumococcal otitis media. Infect Immun **81:**645–652. http://dx.doi.org/10.1128/IAI.01278-12.
17. **Hoffmann E, Stech J, Guan Y, Webster RG, Perez DR.** 2001. Universal primer set for the full-length amplification of all influenza A viruses. Arch Virol **146:**2275–2289. http://dx.doi.org/10.1007/s007050170002.
18. **Tate MD, Brooks AG, Reading PC.** 2011. Specific sites of N-linked glycosylation on the hemagglutinin of H1N1 subtype influenza A virus determine sensitivity to inhibitors of the innate immune system and virulence in mice. J Immunol **187:**1884–1894. http://dx.doi.org/10.4049/jimmunol.1100295.
19. **Wells MA, Albrecht P, Daniel S, Ennis FA.** 1978. Host defense mechanisms against influenza virus: interaction of influenza virus with murine macrophages in vitro. Infect Immun **22:**758–762.
20. **Perrone LA, Plowden JK, Garcia-Sastre A, Katz JM, Tumpey TM.** 2008. H5N1 and 1918 pandemic influenza virus infection results in early and excessive infiltration of macrophages and neutrophils in the

lungs of mice. PLoS Pathog **4:**e1000115. http://dx.doi.org/10.1371/journal.ppat.1000115.
21. **Chan RW, Leung CY, Nicholls JM, Peiris JS, Chan MC.** 2012. Proinflammatory cytokine response and viral replication in mouse bone marrow derived macrophages infected with influenza H1N1 and H5N1 viruses. PLoS One **7:**e51057. http://dx.doi.org/10.1371/journal.pone.0051057.
22. **Gong J, Xu W, Zhang J.** 2007. Structure and functions of influenza virus neuraminidase. Curr Med Chem **14:**113–122. http://dx.doi.org/10.2174/092986707779313444.
23. **Amorim MJ, Bruce EA, Read EK, Foeglein A, Mahen R, Stuart AD, Digard P.** 2011. A Rab11- and microtubule-dependent mechanism for cytoplasmic transport of influenza A virus viral RNA. J Virol **85:**4143–4156. http://dx.doi.org/10.1128/JVI.02606-10.
24. **Tate MD, Brooks AG, Reading PC.** 2011. Correlation between sialic acid expression and infection of murine macrophages by different strains of influenza virus. Microbes Infect **13:**202–207. http://dx.doi.org/10.1016/j.micinf.2010.10.004.
25. **Lohmeyer J, Talens LT, Klenk HD.** 1979. Biosynthesis of the influenza virus envelope in abortive infection. J Gen Virol **42:**73–88.
26. **Lau SC, Scholtissek C.** 1995. Abortive infection of Vero cells by an influenza A virus (FPV). Virology **212:**225–231. http://dx.doi.org/10.1006/viro.1995.1473.
27. **Veit M, Serebryakova MV, Kordyukova LV.** 2013. Palmitoylation of influenza virus proteins. Biochem Soc Trans **41:**50–55. http://dx.doi.org/10.1042/BST20120210.
28. **Tate MD, Job ER, Deng YM, Gunalan V, Maurer-Stroh S, Reading PC.** 2014. Playing hide and seek: how glycosylation of the influenza virus hemagglutinin can modulate the immune response to infection. Viruses **6:**1294–1316. http://dx.doi.org/10.3390/v6031294.
29. **Pal S, Santos A, Rosas JM, Ortiz-Guzman J, Rosas-Acosta G.** 2011. Influenza A virus interacts extensively with the cellular SUMOylation system during infection. Virus Res **158:**12–27. http://dx.doi.org/10.1016/j.virusres.2011.02.017.
30. **Regan JF, Liang Y, Parslow TG.** 2006. Defective assembly of influenza A virus due to a mutation in the polymerase subunit PA. J Virol **80:**252–261. http://dx.doi.org/10.1128/JVI.80.1.252-261.2006.
31. **McAuley JL, Zhang K, McCullers JA.** 2010. The effects of influenza A virus PB1-F2 protein on polymerase activity are strain specific and do not impact pathogenesis. J Virol **84:**558–564. http://dx.doi.org/10.1128/JVI.01785-09.
32. **Mazur I, Anhlan D, Mitzner D, Wixler L, Schubert U, Ludwig S.** 2008. The proapoptotic influenza A virus protein PB1-F2 regulates viral polymerase activity by interaction with the PB1 protein. Cell Microbiol **10:**1140–1152. http://dx.doi.org/10.1111/j.1462-5822.2008.01116.x.
33. **Rossman JS, Lamb RA.** 2011. Influenza virus assembly and budding. Virology **411:**229–236. http://dx.doi.org/10.1016/j.virol.2010.12.003.
34. **Gujuluva CN, Kundu A, Murti KG, Nayak DP.** 1994. Abortive replication of influenza virus A/WSN/33 in HeLa229 cells: defective viral entry and budding processes. Virology **204:**491–505. http://dx.doi.org/10.1006/viro.1994.1563.
35. **Xiao H, Killip MJ, Staeheli P, Randall RE, Jackson D.** 2013. The human interferon-induced MxA protein inhibits early stages of influenza A virus infection by retaining the incoming viral genome in the cytoplasm. J Virol **87:**13053–13058. http://dx.doi.org/10.1128/JVI.02220-13.
36. **Pavlovic J, Zurcher T, Haller O, Staeheli P.** 1990. Resistance to influenza virus and vesicular stomatitis virus conferred by expression of human MxA protein. J Virol **64:**3370–3375.
37. **Siegrist F, Ebeling M, Certa U.** 2011. The small interferon-induced transmembrane genes and proteins. J Interferon Cytokine Res **31:**183–197. http://dx.doi.org/10.1089/jir.2010.0112.
38. **Feeley EM, Sims JS, John SP, Chin CR, Pertel T, Chen LM, Gaiha GD, Ryan BJ, Donis RO, Elledge SJ, Brass AL.** 2011. IFITM3 inhibits influenza A virus infection by preventing cytosolic entry. PLoS Pathog **7:**e1002337. http://dx.doi.org/10.1371/journal.ppat.1002337.
39. **Winkler M, Bertram S, Gnirss K, Nehlmeier I, Gawanbacht A, Kirchhoff F, Ehrhardt C, Ludwig S, Kiene M, Moldenhauer AS, Goedecke U, Karsten CB, Kuhl A, Pohlmann S.** 2012. Influenza A virus does not encode a tetherin antagonist with Vpu-like activity and induces IFN-dependent tetherin expression in infected cells. PLoS One **7:**e43337. http://dx.doi.org/10.1371/journal.pone.0043337.
40. **Watanabe R, Leser GP, Lamb RA.** 2011. Influenza virus is not restricted by tetherin whereas influenza VLP production is restricted by tetherin. Virology **417:**50–56. http://dx.doi.org/10.1016/j.virol.2011.05.006.
41. **Wang J, Nikrad MP, Travanty EA, Zhou B, Phang T, Gao B, Alford T, Ito Y, Nahreini P, Hartshorn K, Wentworth D, Dinarello CA, Mason RJ.** 2012. Innate immune response of human alveolar macrophages during influenza A infection. PLoS One **7:**e29879. http://dx.doi.org/10.1371/journal.pone.0029879.
42. **Allen IC, Scull MA, Moore CB, Holl EK, McElvania-TeKippe E, Taxman DJ, Guthrie EH, Pickles RJ, Ting JP.** 2009. The NLRP3 inflammasome mediates in vivo innate immunity to influenza A virus through recognition of viral RNA. Immunity **30:**556–565. http://dx.doi.org/10.1016/j.immuni.2009.02.005.
43. **Szretter KJ, Brien JD, Thackray LB, Virgin HW, Cresswell P, Diamond MS.** 2011. The interferon-inducible gene viperin restricts West Nile virus pathogenesis. J Virol **85:**11557–11566. http://dx.doi.org/10.1128/JVI.05519-11.
44. **Cho H, Proll SC, Szretter KJ, Katze MG, Gale M, Jr, Diamond MS.** 2013. Differential innate immune response programs in neuronal subtypes determine susceptibility to infection in the brain by positive-stranded RNA viruses. Nat Med **19:**458–464. http://dx.doi.org/10.1038/nm.3108.